FAST DESIGN METHODOLOGY FOR SUPERSONIC ROTOR BLADES WITH DENSE GAS EFFECTS

Elio Antonio Bufi[1], Benoit Obert[2], Paola Cinnella[3*]

[1] Laboratoire DynFluid
Arts et Metiers ParisTech, Paris (France)
Polytechnic of Bari, Bari (Italy)
Email: elio-antonio.bufi@ensam.eu

[2] ENERTIME, Courbevoie (France)
Email: benoit.obert@enertime.com

[3] Arts et Metiers ParisTech, Paris (France)
Email: paola.cinnella@ensam.eu

* Corresponding Author

ABSTRACT

This work describes a fast 2-D design methodology based on the method of characteristics (MOC) for rotor blade vanes of supersonic axial Organic Rankine Cycle (ORC) impulse expanders. The MOC is generalized to gases governed by complex equations of state to fully account for dense gas behavior characteristic of ORC turbines. The fluid thermodynamic properties are described by highly accurate multiparameter equations of state based on Helmholtz free energy. Several working fluids are considered, including R245fa, R134a, R227ea, R236fa. The designs generated by the generalized MOC are compared with those obtained under the classical perfect gas model. Finally, CFD simulations of both isolated rotor blades and a full turbine stage are carried out to assess the performance of the designs using the ANSYS CFX solver.

1. INTRODUCTION

In recent years, the Organic Rankine Cycle (ORC) technology has received great interest from the scientific and technical community because of its capability of generating electric power using low temperature sources with good performances. For compactness, mechanical design simplicity and cost reasons, ORC plants often use single stage expander characterized by high pressure ratios, which leads to supersonic flow conditions. Furthermore, ORC working fluids are often characterized by the so-called dense-gas effects (see, e.g. (Congedo et al., 2011) and references cited therein).
The gas dynamics of dense gases can be described through a key thermodynamic property, known as the fundamental derivative of gas dynamics (Thompson, 1971):

$$\Gamma = 1 + \frac{\rho}{a}\left(\frac{\partial a}{\partial \rho}\right)_s \tag{1}$$

Equation (1) represents a measure of the rate of change for the local speed of sound with respect to density in isentropic transformation (Colonna et al., 2009). For light fluids, $\Gamma > 1$. This is the case of perfect gases, which have a constant $\Gamma = (\gamma + 1)/2$.
For fluid with sufficient molecular complexity and under specific thermodynamic conditions, $\Gamma < 1$, which leads to a reverse behaviour of the speed of sound in isentropic perturbations with respect to classical case: a decreases in isentropic compressions and grows in isentropic expansions.
The aerodynamic modelling of such a system is made difficult by dense gas effects characterizing the thermodynamic behaviour of the working fluid in the vicinity of the critical point and the saturation curve.

The need for a compact turbine working with high pressure ratios implies the choice of an impulse turbine architecture. This can be justified by considering a typical impulse blade and its velocity triangle (figure 4).

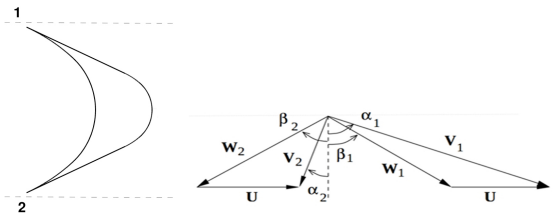

Figure 1: Example of impulse blade geometry and velocity triangles

By imposing an axial outlet flow for the impeller ($\alpha_2 = 0$), with the axial absolute velocity component kept constant, the work coefficient can be expressed as:

$$\psi = \frac{\Delta H_0}{U^2} = 2(1 - \Lambda) \tag{2}$$

In equation (2), U represents the peripheral velocity at a specified radius, ΔH_0 the total enthalpy drop per unit mass across the impeller and Λ the degree of reaction. For an impulse turbine ($\Lambda = 0$), the total enthalpy drop is two times greater than for a 0.5 reaction degree turbine. This property allows extracting a large amount of work from a single stage, with a maximum for a vane outlet swirl equal to 67° and rotor turning to 116° ($\beta_1 = \beta_2 = 58°$) (Paniagua et al., 2014). However, particular care must be addressed to the rotor and stator blades aerodynamic design because both behave as supersonic nozzles. Moreover, the typical operating conditions for an ORC turbine are in the proximity of the working fluid saturation curve or sometimes supercritical. Due to the presence of strong dense gas effects, models used to design the blade shapes have to be modified accordingly. Several authors in the past have addressed the design of dense gas nozzles and stator blades (Cramer and Tarkenton, 1992; Guardone et al., 2013; Wheeler and Ong, 2013; Bufi et al., 2015). All of them generally rely on extended versions of the Method of Characteristics (MOC) for 2D supersonic flows. The aim of this work is to develop, for the first time to the Authors knowledge, a methodology for the design of rotor blades of axial supersonic ORC impulse turbines, which takes properly into account dense gas effects. This is based on the MOC along with the vortex flow field approach, previously introduced for perfect gas flows (Goldman, 1968; Paniagua et al., 2014), extended to the dense gas case.

The performances of blade shapes obtained with MOC using different organic working fluids are then evaluated by means of numerical simulations carried out using the ANSYS CFX code, both for the isolated rows and for a supersonic turbine stage.

2. SUPERSONIC IMPULSE TURBINE BLADES DESIGN

In this Section we first recall the Method of Characteristics (MOC) for the design of perfect gas supersonic nozzles and its extension to dense gas flows. Then, we present its application to the design of supersonic rotor blades, in conjunction with a free-vortex methodology.

2.1 MOC for supersonic nozzle design

The MOC is a classical method for the design of the divergent part of supersonic nozzles under the hypotheses of 2D, steady and homentropic flow. Such a flow is governed by the 2D isentropic Euler equations, which represent an hyperbolic system of conservation laws characterized by two families of characteristic lines. These are defined by equations of the form (Délery, 2010; Zucrow and Hoffman, 1976):

$$\frac{dy}{dx} = tan(\varphi \mp \mu) \tag{3}$$

where φ is the local flow angle and $\mu = arcsin(M^{-1})$ is the Mach angle. Rewriting the governing equations in the characteristic reference frame, one gets the so-called compatibility equations, which are just ordinary differential equations, of the form:

$$d\varphi \pm \sqrt{M^2 - 1}\frac{dV}{V} = 0 \tag{4}$$

where V is the velocity magnitude and the sign + or − denotes a left-running or − a right-running characteristic line, respectively. For a perfect gas, equations (4) can be integrated analytically after rewriting dV/V in terms of the Mach number and by making use of the equation of state, leading to the well-known Prandtl-Meyer relations:

$$\varphi \pm \nu(M) = constant \text{ (along a characteristic)} \tag{5}$$

The preceding equations, along with the equations of the characteristic lines (3) are then used as described in (Délery, 2010) to design the nozzle wall contour. In the case of a dense gas, equation (4) can no longer be integrated analytically. Instead, we use a numerical method for ordinary differential equations, namely, Heun's second-order predictor-corrector method to carry out the integration along characteristic lines. The discretized compatibility equation is supplemented by dense gas equations of state to compute all of the required thermodynamic properties. Precisely, we make use of the thermodynamic library REFPROP (Lemmon et al., 2013), which contains reference multiparameter equations of state for many dense gases of potential interest as ORC working fluids. Extensions of the MOC to dense gases were proposed in the past by (Guardone et al., 2013; Wheeler and Ong, 2013) with focus on the design of De-Laval nozzles or radial turbine injectors, respectively. In (Bufi et al., 2015) the methodology is extended to dense gas models by using reference EOS and applied to axial turbomachinery design.
Once the nozzle divergent has been designed via the MOC, a geometrical postprocessing procedure is applied to generate a supersonic turbine nozzle. Some geometrical parameters are imposed in order to control the final blade geometry (see figure 2): the stagger angle θ, the angular extension Φ and the radius of the leading edge arc *cb*, the radius *R* of the leading edge arc *cd* and the trailing edge thickness *ef*.

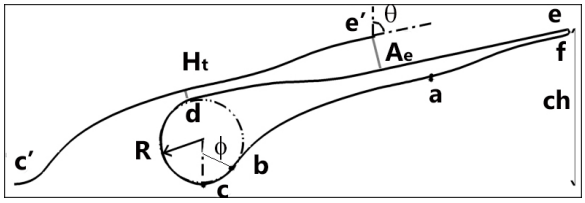

Figure 2: Example of supersonic stator blade geometry designed with MOC.

2.2 Design of dense gas supersonic rotor blades

For the design of supersonic rotor blades we follow the procedure described in (Paniagua et al., 2014; Goldman, 1968) for perfect gas flows and we extend it to dense gases.
The flow at the rotor inlet is assumed as a uniform one that is simply deflected by the rotor blades. To achieve this deflection, the flow passes through a transition region delimited by upper and lower transition arcs and by characteristic lines. For clarity, the transition region is sketched in figure 3, where AB and CD are transition arcs and the dashed lines are used to represent the characteristics. Through this region, the uniform inlet flow is converted into a free vortex flow, for which $V \cdot R = constant$, with R the radius of curvature of a streamline and V the constant velocity along it, following an isentropic transformation.
Figure 4 shows a schematic description of the rotor blade geometry designed with MOC. We use the same notation of the MOC for perfect gases reported in (Paniagua et al., 2014; Goldman, 1968) and we refer to them for details. In order to start with the design procedure for dense gases, the following input parameters are defined: inlet total pressure and temperature; inlet/outlet relative flow angle β_i/β_o;

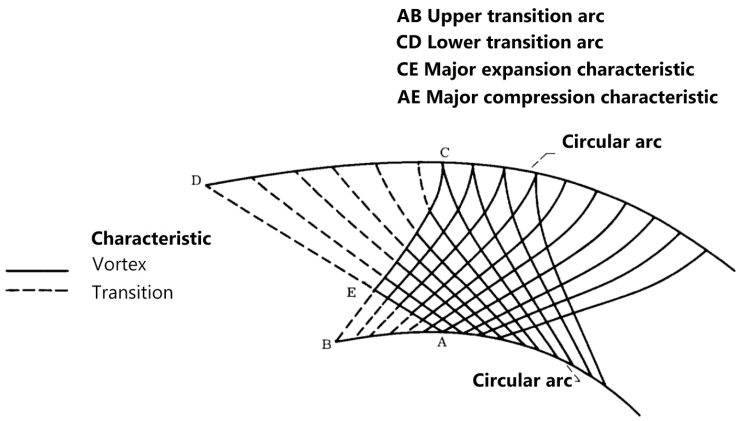

Figure 3: Scheme of the system of characteristic lines in the rotor vane. (Goldman, 1968)

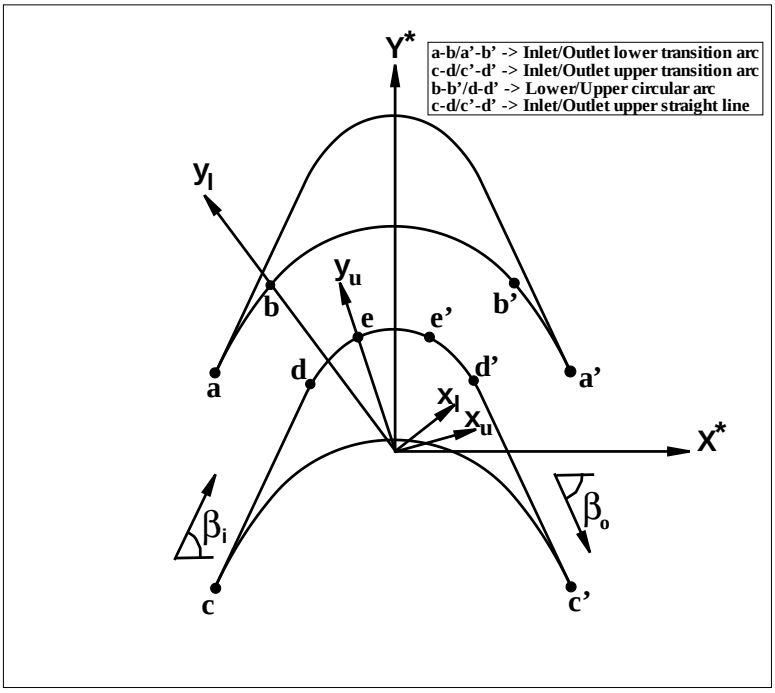

Figure 4: Schematic description of the rotor blade design.

inlet/outlet Mach number M_i/M_o; the lower arc Mach number M_l, assigned on the lower circular arc b-b'; the upper arc Mach number M_u, assigned on the upper circular arc d-d'. As for the perfect gas model, the lower and upper transition arcs (a-b/a'-b' and d-e/d'-e' for inlet and outlet, respectively) are determined in the unrotated lower/upper reference systems (denoted with subscripts l and u). The geometry is then rotated in the $X^* - Y^*$ reference system and completed with the straight line parts c-d/c'-d' and the circular arcs b-b'/d-d'.

The MOC for perfect gas algorithm makes use of the analytical expressions of the Prandtl-Meyer function $\nu = \nu(M)$ and of the critical Mach number $M^* = M^*(M)$ (with $M^* = V/a^*$ and a^* the critical speed of sound) for perfect gases. For a dense gas, no such analytical expressions are available.

The calculation of the critical Mach number is replaced by the following iterative procedure:

1. The critical speed of sound is first computed from the known values of the total pressure p_0 and temperature T_0 by using a thermodynamic library available in REFPROP
2. An initial tentative value $M^{*(0)}$ for the critical Mach number is prescribed.
3. At each iteration of the method, an updated value of the velocity magnitude is computed as $V^{(m)} =$

$M^{*(m-1)}a^*$

4. The latter is used to compute an updated value of the specific static enthalpy $h^{(m)}$, given the total enthalpy $h_0 = h_0(p_0, T_0)$.
5. The speed of sound is then updated by using the thermodynamic relation $a^{(m)} = f(h^{(m)}, s)$, where the entropy s is constant everywhere and is known from the prescribed inlet conditions.
6. Finally, an updated value of the Mach number $M^{(m)} = V^{(m)}/a^{(m)}$ is obtained.
7. If $M^{(m)} - M^{(m-1)}$ is below a given tolerance, the procedure is stopped. Otherwhise, a new value is assigned for $M^{*(m+1)}$ (by using a bisection procedure) and the iteration is started again.

The design procedure above is completed by adding a finite leading-edge/trailing-edge thickness. Besides, non-symmetrical blades with various degrees of reaction can be designed if different inlet/outlet input parameters are imposed. In this work, unique incidence problems related to the supersonic relative flow on the rotor inlet are neglected on design stage, due to the interest on viscous effects which could make useless any incidence angle calculation based on inviscid theory.

2.3 Example of rotor blade designs

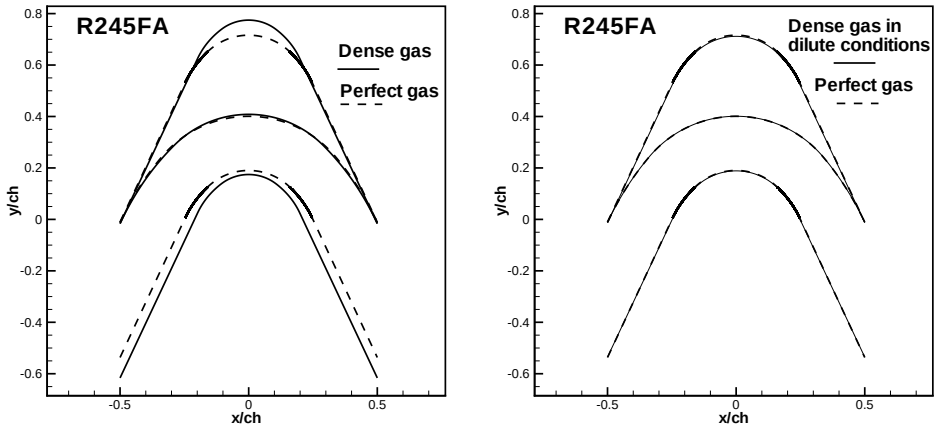

(a) (b)

Figure 5: Blade designs for R245FA at operating conditions ($p_r^0 = 1.05, T_r^0 = 1.05$) (a) and at conditions ($p_r^0 = 0.055, T_r^0 = 1.15$)(b). Dashed lines represent designs obtained under the perfect gas model.

Four organic working fluids are used to test the MOC. Their critical properties are shown in table 1, where γ is the specific heat ratio in the dilute gas limit along the critical isotherm curve (Guardone et al., 2013). The design algorithm for rotor blades has been run for a typical ORC working fluid, namely

Table 1: Thermophysical properties for different organic substances, based on reference EOS (from REFPROP ver. 9.1).

	R245fa	**R227ea**	**R134a**	**R236fa**
$p_c[MPa]$	3.651	2.93	4.06	3.2
$T_c[K]$	427.16	374.9	374.2	398.07
$\rho_c[kg/m^3]$	516.08	594.2	511.9	551.3
$M_w[g/mol]$	134.05	170.03	102.03	152.04
γ	1.061	1.056	1.092	1.059

R245FA, whose thermophysical properties are given in table 1 and used to investigate the impact of real gas effects on the resulting geometry. The degree of reaction is set to zero, so that the resulting geometry is symmetric. Figure 5 shows a comparison of geometries calculated with different operating

conditions and gas models. The first operation point (characterised by the reduced pressure p_r^0 = 1.05 and the reduced temperature T_r^0 = 1.05) is very close to the R245FA upper saturation curve and this affects the rotor geometry, leading to larger cross section variations with respect to perfect gas. Indeed, a greater generic area to throat area ratio is addressed to the REF geometry. This is a typical behavior already seen in supersonic stators (Guardone et al., 2013). It is due to the effect of Γ that, being lower than one in dense gas regions, provides higher exit-to-throat area ratios.
Figure 5b shows the design obtained for a lower total pressure (p_r^0 = 0.055) and higher total temperature (T_r^0 = 1.15), so that the thermodynamic conditions at rotor inlet lie far from the dese gas region. Here, the blade designed with a dense gas EOS is very similar to that obtained with the perfect gas model. Then,

Table 2: Geometrical output parameters for four different organic fluids under the same operating condition (p_r^0 = 1.28, T_r^0 = 1.28, M_{in} = M_{out} = 1.5, M_l = 1, M_u = 2 ,β_{in} = β_{out} = 65°).

	R245fa	**R227ea**	**R134a**	**R236fa**
σ	1.82	1.81	1.85	1.82
ch^*	2.31	2.32	2.30	2.31
ph^*	1.27	1.28	1.24	1.27

a parametric study for several working fluids suitable for ORC applications at the same reduced input conditions has been carried out. Fluid properties are also given in table 1. For all of the fluids, the input thermodynamic conditions and design parameters are set to (p_r^0 = 1.28, T_r^0 = 1.28, M_{in} = M_{out} = 1.5, M_l = 1, M_u = 2 ,β_i = β_o = 65°). Table 2 provides the following geometrical parameters for the resulting designs: blade solidity σ, defined as the axial chord to pitch ratio; the axial chord ch^* and pitch ph^* normalized respect to the critic radius r^*, the latter defined as the radius of the sonic streamline in the vortex flow field. It can be noticed that the lower is the fluid molecular complexity (as for the R134A fluid) the higher is the solidity.

3. NUMERICAL SIMULATIONS

Viscous 2-D numerical simulations have been carried out for both an isolated rotor blade row and a full turbine stage designed using the MOC methods presented in this paper. The CFD software used is the commercial code Ansys CFX 16.0. The turbulence model used is k-omega SST (Shear Stress Transport). The thermodynamic properties of the fluids are modelled using the real gas properties (rgp) library (ANSYS, 2015). The rgp files contain property tables mapped as a function of temperature and pressure along the turbine expansion and allow accurately taking into account dense gas effects.
In table 3 the parameters used to design the blade shapes and to perform the simulations with the R245FA working fluid are shown. In order to assess the presence of dense gas effects it is important to evalu-

Table 3: Rotor blade design parameters.

Parameters	Values
Inlet total relative pressure [bar]	6
Inlet total relative temperature [K]	393.15
Inlet relative Mach number	1.5
Inlet relative flow angle [°]	60
Suction side circular arc Mach number	1.9
Pressure side circular arc Mach number	1.1

ate the position of the operating point on the working fluid state diagram. In figure 6a the isentropic evolution of the expansion on the T-S diagram is shown. The presence of strong dense gas effects is expected, since fundamental derivative Γ is below 1 throughout the expansion (see figure 6b). It can be noticed that, for this application, the strongest dense gas effects occur mainly inside the nozzle, where

the enthalpy drop is elaborated. This is due to the "dry" nature of R245FA fluid which allows to have the last part of expansion farther from the saturation curve. Simulations for an isolated supersonic rotor

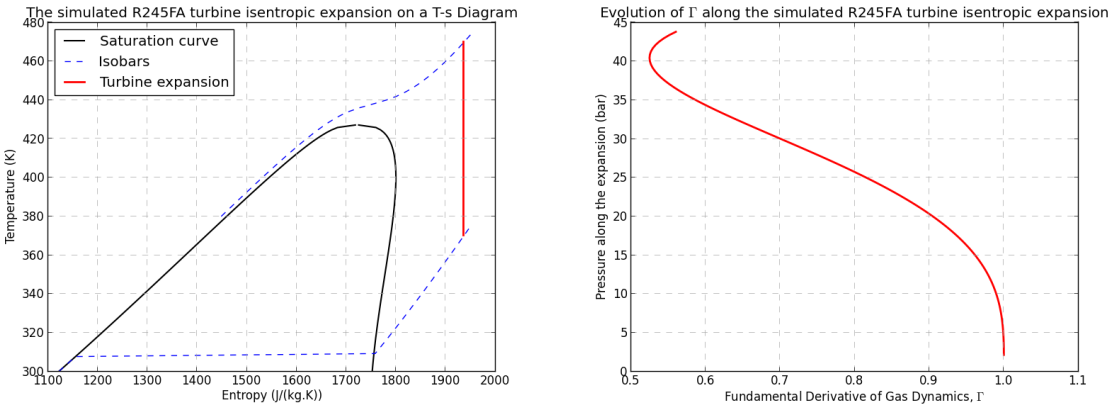

(a) (b)

Figure 6: Isentropic turbine expansion on the R245FA T-S diagram (a); Fundamental Derivative of gas dynamics Γ evaluated along the turbine expansion (b).

blade row using fluid R245FA have been carried out in the relative reference system. The blade row considered is symmetric, so the outlet conditions are identical to the inlet conditions. The inlet rotor angle is prescribed according to the stator exit conditions.

By using the Zweifel empirical coefficient (Zweifel, 1945), the number of rotor to stator blades ratio is set to 2. The 2-D computational grid for the full stage simulation is composed of C-shaped blocks around the blades and of H-shaped blocks at stage inlet and outlet shown in figure 7a. It is generated using Ansys TurboGrid and refined to obtain y+ values less than 1 at the blade walls with 330066 total number of elements (121704 overall elements for the rotor row and 208362 elements for the stator row). Simulations for a full turbine stage involving a supersonic rotor blade row and a supersonic stator blade row both designed by the means of the MOC procedures presented in this paper are carried out. The total temperature, the total pressure and the velocity components are imposed at the inlet. Average static pressure is set at the outlet and a mixing-plane boundary condition is set at the stator-rotor interface. Table 4 presents the main turbine working parameters, taken from a real-world application (they are different from those used in the previous section 2.4). In order to maximize the impact of dense gas effects, we choose supercritical turbine inlet conditions (see figure 6a). Only the results for R245FA fluid are shown because of the absence of substantial differences among the other fluids considered in this paper (see table 1). Figure 7b presents the relative Mach number distribution for the full turbine stage simulation. The flow is accelerated in the stator vanes up to the design absolute Mach number of 2.4 and, thanks to the accurate design with the MOC algorithm, no normal shocks are formed in the divergent part of the nozzle. Thanks to the accurate design with the MOC algorithm, no normal shocks are formed in the divergent part of the nozzle. However, weak oblique shocks are generated at the trailing edge of the stator due the rounded trailing edge. These shocks interact with the viscous wake, visible on the stator outlet. Due to the mixing plane interface, interactions of the latter with the rotor row can not be observed. The flow in the rotor vanes is characterised by weak oblique shocks departing both from the leading and trailing edge of the blades due to the finite thickness of the actual rotor geometry. The turbine is found to be in a "started" configuration, since a normal shock at the inlet is avoided and the flow inside the rotor vanes is supersonic (Kantrowitz et al., 1945). The flow in the relative reference frame is then deflected by the blade vanes up to a relative Mach number slightly lower than the design one due to the set of oblique shocks departing both from leading and trailing edge. To better analyse the flow behaviour in the rotor vanes an isolated rotor simulation has been performed (see figure 8b). At the inlet of the rotor vanes, the presence of an oblique shock wave is noticed. Two oblique shocks depart also from trailing

edge: one impinges the suction side while the other one interacts with the viscous wake. The careful design of the rotor blade prevents the formation of a normal shock at the inlet that would slow down the flow to subsonic conditions within the blade passage. The calculated total to total isentropic efficiency for this turbine is 92.9%. In order to assess the main source of losses in the turbine stage, it is useful to analyse the entropy deviation $(S-S_{in})/S_{in}$, with S_{in} the specific entropy at inlet. The entropy deviation is shown in figure 8a for the isolated rotor. Entropy is mainly generated with the viscous boundary layers and wakes, whereas entropy generation across shocks is extremely weak. This demonstrates that the proposed methodology provides blade designs with negligible shock losses. The presence of viscous effects also modify the design degree of reaction, set to zero for the design here proposed. The actual degree of reaction evaluated after simulations is found to be 0.042. This effect can be addressed to the modification of the effective blade vane geometry due to the boundary layer thickness, which lead to lower passage sections going from inlet to outlet.

Table 4: Main turbine full stage working parameters.

Parameters	Values
Inlet total reduced pressure	1.2
Pressure ratio	20.6
Inlet total reduced temperature	1.1
Stator nozzle outlet design Mach number	2.4
Stator stager angle [°]	70
Rotor blade speed [m/s]	141.37

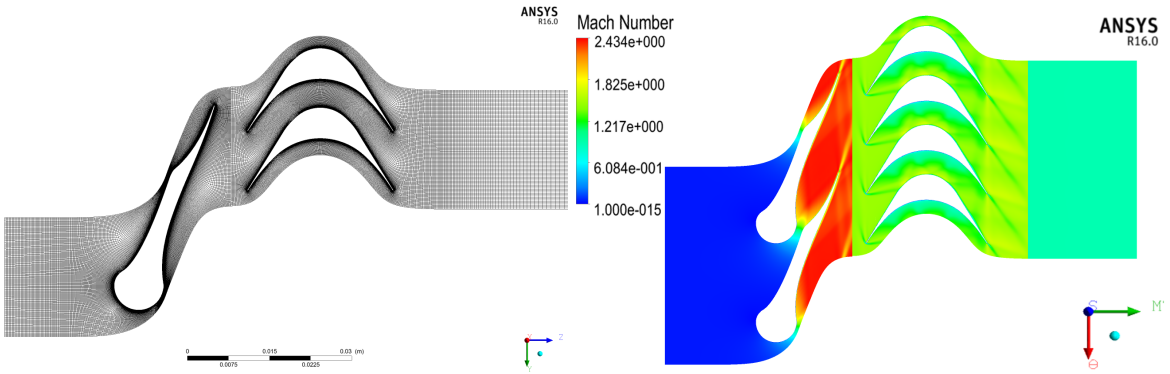

(a) (b)

Figure 7: Computational block structured grid for full turbine stage (330066 elements) (a); relative Mach number distribution for R245FA fluid (b).

4. CONCLUSIONS

An efficient design procedure for supersonic ORC turbine rotor blades taking carefully into account dense gas effects has been developed. It is based on the method of characteristics and allows designing blade vanes by imposing the momentum conservation through a free vortex flow condition. Significant differences are found between geometries obtained with the ideal and dense gas models. The numerical simulations show that the accurate blade design in dense gas flow regime allows accounting for the dense gas phenomena during expansion and avoiding the focusing of characteristic lines into strong right shocks inside the blade vanes. The main source of loss of performances can be then addressed to the viscous phenomena, as confirmed by the entropy deviation analysis.

Future developments of the supersonic ORC turbine stage design process will lead to the unsteady nu-

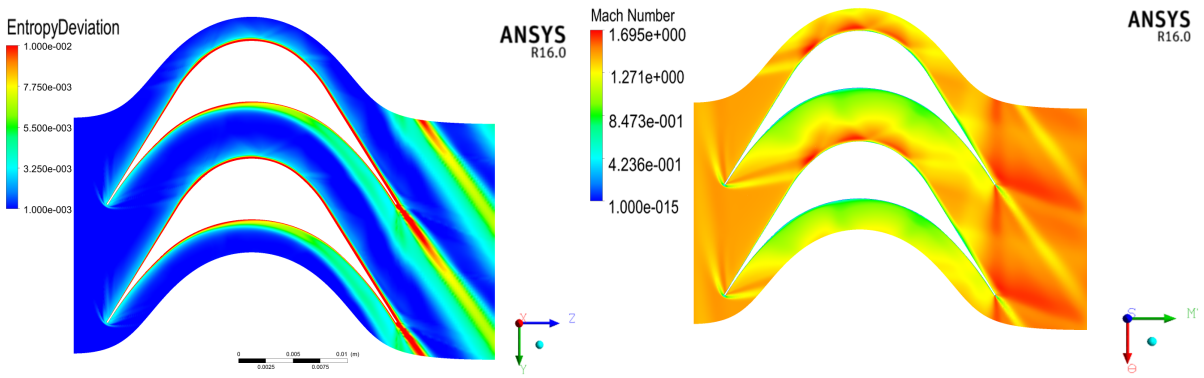

(a) (b)

Figure 8: Entropy deviation contour plot for the isolated rotor (R245FA fluid) (a); Mach number distribution for the isolated rotor (R245FA fluid) (b).

merical analysis of the entire turbine stage in order to take into account the interactions between stator and rotor due to viscous phenomena along with the 3-D turbine full stage design.

ACKNOWLEDGEMENTS

The authors would like to thank ADEME (Agence de l'Environnement et de la Maîtrise de l'Energie), PS2E (Paris-Saclay Efficacité Energétique) and Total who partially funded the works presented in this paper.

REFERENCES

ANSYS, I. (2015). Ansys cfx-solver modeling guide.

Bufi, E. A., Cinnella, P., and Merle, X. (2015). Sensitivity of supersonic orc turbine injector designs to fluctuating operating conditions. *Proceedings of the ASME 2015 Turbo Expo Turbine Technical Conference, ASME TURBO EXPO 2015 June 15-19, 2015, Montreal, Canada (Submitted and accepted)*.

Colonna, P., Nannan, N., Guardone, A., and Van der Stelt, T. (2009). On the computation of the fundamental derivative of gas dynamics using equations of state. *Fluid Phase Equilibria*, 286(1):43--54.

Congedo, P., Corre, C., and Martinez, J.-M. (2011). Shape optimization of an airfoil in a BZT flow with multiple-source uncertainties. 200(1-4):216 -- 232.

Cramer, M. and Tarkenton, G. (1992). Transonic flows of bethe-zel'dovich-thompson fluids. *Journal of Fluid Mechanics*, 240:197--228.

Délery, J. (2010). *Handbook of compressible aerodynamics*. ISTE.

Goldman, L. J. (1968). Analytical investigation of supersonic turbomachinery blading. 1/2-analysis of impulse turbine-blade sections.

Guardone, A., Spinelli, A., and Dossena, V. (2013). Influence of molecular complexity on nozzle design for an organic vapor wind tunnel. *Journal of Engineering for Gas Turbines and Power*, 135(4):042307.

Kantrowitz, A., Donaldson, C., Laboratory, L. A., and for Aeronautics, U. S. N. A. C. (1945). *Preliminary Investigation of Supersonic Diffusers*. National Advisory Committee for Aeronautics.

Lemmon, E. W., Huber, M. L., and McLinden, M. O. (2013). *NIST Reference Fluid Thermodynamic and Transport Properties - REFPROP Version 9.1*. NIST.

Paniagua, G., Iorio, M., Vinha, N., and Sousa, J. (2014). Design and analysis of pioneering high supersonic axial turbines. *International Journal of Mechanical Sciences*, 89:65--77.

Thompson, P. A. (1971). A fundamental derivative in gasdynamics. *Physics of Fluids (1958-1988)*, 14(9):1843--1849.

Wheeler, A. P. and Ong, J. (2013). The role of dense gas dynamics on orc turbine performance. In *ASME Turbo Expo 2013: Turbine Technical Conference and Exposition*, pages V002T07A030--V002T07A030. American Society of Mechanical Engineers.

Zucrow, M. J. and Hoffman, J. D. (1976). Gas dynamics. *New York: Wiley, 1976*, 1--2.

Zweifel, O. (1945). The spacing of turbomachine blading, especially with large angular deflection. *Brown Bovery Review 32*.

NOMENCLATURE

a	Speed of sound	(m/s)
ch	Axial chord	(m)
p	Pressure	(Pa)
ph	Blade pitch	(m)
G	Mass-flow rate	(kg/s)
H	Specific enthalpy	(J/kg)
M	Mach number	
R	Radius for the design of the convergent	(m)
R_g	Specific gas constant	$(J/kg * K)$
S	Specific entropy	$(J/kg * K)$
T	Temperature	(K)
V	Velocity	(m/s)
β_a	Leading edge attach angle	(rad)
γ	Specific heat ratio	
η_{is}	Isentropic efficiency	
θ	Stagger angle	(rad)
μ	Mach angle	(rad)
ν	Prandtl-Meyer function	
v_s	Specific volume	(m^3/kg)
ρ	Density	(kg/m^3)
σ	Blade solidity (chord to pitch ratio)	
φ	Flow angle	(rad)
Φ	Leading edge angular extension.	(rad)

Subscript

r	Reduced: normalised respect to critical conditions.
c	Critical thermodynamic property.
0	Total/reservoir thermodynamic property.

Superscript

$*$	Critic (sonic) parameter.

Acronyms/abbreviations

MOC	Method Of Characteristics.
REF	REFPROP model.
EOS	Equation Of State.
CFD	Computational Fluid Dynamics.
ORC	Organic Rankine Cycle.